Control Architecture for a Doubly-fed Induction Machine Propulsion Drive

Arijit Banerjee, Michael S. Tomovich, Steven B. Leeb and James L. Kirtley
Department of Electrical Engineering and Computer Science, Massachusetts Institute of Technology
Cambridge, Massachusetts, USA
arijit@mit.edu, tomovich@mit.edu, sbleeb@mit.edu, kirtley@mit.edu

Abstract—**This paper presents a control architecture for a Doubly-Fed Induction Machine (DFIM) intended for propulsion applications. The DFIM is a mainstay for windmill and renewable energy applications. A unique controller is needed to fit the different demands of transportation applications, specifically where both AC and DC supply are available. This will enable increased range of operating speed with minimum power electronics on board. Compared to a wind turbine application, added challenges in a propulsion application are sudden load variations and the need for robust control during these variations. In this case, a shipboard application is examined.**

Keywords- Doubly fed induction machine (DFIM), propulsion drive, stator flux oriented control, stator flux estimation, synchronizer, reactive power control

I. NOMENCLATURE

ε	: Rotor A-phase angle w.r.t stator A-phase axis (radians)
$\overline{I_s}$, $\overline{I_r}$	: Stator and rotor current space vector (A)
J, B	: Total Inertia (kgm^2) & Frictional coefficient (Nm-s/rad)
K_d	: Feedback damping gain in AC transition flux controller
P	: Number of poles
R_s, R_r	: Stator and rotor resistances (Ohms)
Sw	: Switching signal for AC-DC mode changeover
τ, T_L	: Electromagnetic and Load torque (N-m)
$\overline{V_{ac}}$, $\overline{V_{dc}}$	: AC and DC voltage space vector (V)
$\overline{V_s}$, $\overline{V_r}$	: Stator and rotor voltage space vector (V)
ω, ω_e	: Rotor speed in mech. rad/s and in elec. rad/s
ω_s, ω_{ac}	: Stator flux frequency & AC supply frequency (rad/s)
δ	: Angle between ref. frame rotating at ω_{ac} & ω_s
$\overline{\psi_s}$, $\overline{\psi_r}$	: Stator and rotor flux space vector (Wb-Turn)
$\psi_{s\alpha}$, $\psi_{s\beta}$	: Stator flux components in α-β ref. frame (Wb-Turn)
ψ_s, θ_s	: Stator flux mag. $[\sqrt{(\psi_{s\alpha}^2 + \psi_{s\beta}^2)}]$ (Wb-Turn) & angle $[\tan^{-1}(\psi_{s\beta}/\psi_{s\beta})]$ w.r.t stator A-phase (radians)
X_d, X_q	: d and q axis components of any space vector $\overline{X}$
X*	: Reference value of variable X

II. INTRODUCTION

Conventional variable speed drives typically operate from a DC bus. That is, an inverter controls and operates an electric machine by consuming and shaping power from a DC bus. When DC input power is naturally available, e.g., in an electrical vehicle where batteries or a fuel-cell may serve as a storage source, this approach can be attractive. For transportation systems with AC generation [1], and where AC power is desirable for other loads besides motive power (e.g., on a ship), providing a DC bus for a variable speed drive can be a daunting proposition. This approach requires total conversion of the ship's generated power to DC, and then reconstruction of variable AC waveforms using an inverter. A significant investment in power electronics is required, not only for the inverter bus also for the power-factor corrected rectifier likely needed to interface to the AC generator.

A Doubly-fed Induction Machine (DFIM) offers a way to construct a variable speed drive without processing every joule of shaft power from a DC bus. DFIMs are predominantly used in wind power generation [2] and in flywheel energy storage applications [3]. These applications have a reduced speed range that enables processing of rated power through rotor side control using a reduced size power electronics converter. In contrast, a propulsion DFIM has to operate for the complete speed range of the machine. To increase the speed range of a DFIM, it can be fed with controlled double inverters from both the stator and the rotor to obtain rated torque at all speeds [4-5]. Although this has the advantage of having complete control on both the stator and rotor, it calls for more power electronics sizing.

Reference [6] proposes a configuration of a DFIM drive for a ship propulsion application that shows considerable advantages in power electronics required for operation over the complete speed range of the machine. The drive has two sources (AC and DC), either one of which can be connected to the stator winding. The rotor is connected to a power electronic inverter that can make variable frequency waveforms. Figure 1 shows the proposed drive. The stator connects to DC or AC through a switch. In DC or low speed mode - in which the stator is connected to the DC supply - the DFIM behaves like a separately excited synchronous machine. In AC or high speed mode - in which the stator is connected to the AC supply – the machine behaves like a standard DFIM analogous to a windmill generator. A transition between the modes can be made as the machine accelerates. This transition speed can be chosen such that minimum rotor power electronics can control the drive across the complete speed range.

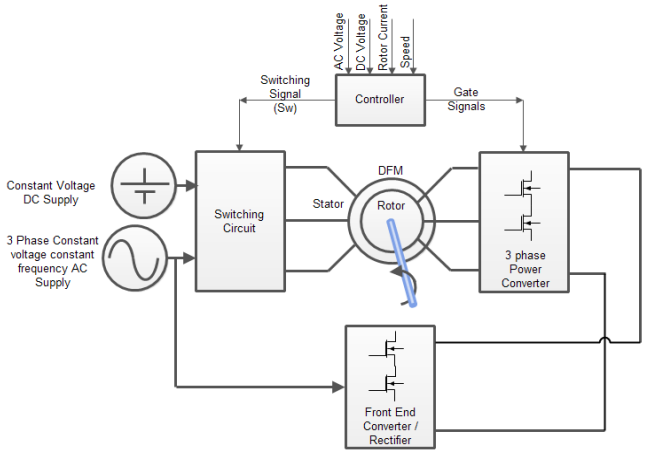

Figure 1. Proposed confirguration of DFIM drive

While extensive literature exists for control of a DFIM for wind applications [7-8], the propulsion configuration has significantly different requirements, including the need to operate with DC flux on the stator at low speed. The propulsion DFIM requires stator flux estimation under any operating conditions as well as smooth transition between operating modes. As with all indirect flux oriented controllers, there is a strong need to accurately estimate and update machine parameters in the control algorithm during operation. In a propulsion application, a control scheme is necessary to properly transition the stator excitation and control the speed of the drive bumplessly through the transition. All of this must work in the context of a propulsion load that can experience sudden disturbances of full per-unit load torque. Finally, the DFIM is capable of being operated to control its reactive power demand in the high speed mode. This is a modeling and control challenge, but also an opportunity. The propulsion DFIM can serve as a drive that can provide controllable power factor to an AC grid or microgrid. This paper discusses the proposed configuration of a DFIM for propulsion applications with specific attention to these and other concerns.

III. DFIM MODEL IN STATOR FLUX ORIENTATION

For the complete analysis and development of the control architecture, a standard DFIM machine model using the space vector approach [9] is used as described by (1-6). While (1-2) are in the stationary reference frame, (3-4) are in the rotor reference frame and (5) is the associated torque expression. (6) denotes a simplified mechanical equation.

$$\overline{V_s} = R_s \overline{I_s} + \frac{d}{dt}\overline{\psi_s} \tag{1}$$

$$\overline{\psi_s} = L_s \overline{I_s} + M \overline{I_r} e^{j\varepsilon} \tag{2}$$

$$\overline{V_r} = R_r \overline{I_r} + \frac{d}{dt}\overline{\psi_r} \tag{3}$$

$$\overline{\psi_r} = L_r \overline{I_r} + M \overline{I_s} e^{-j\varepsilon} \tag{4}$$

$$\tau = \frac{2}{3} M \,\mathrm{Im}\left[\overline{I_s}\left(\overline{I_r} e^{j\varepsilon}\right)^*\right] \tag{5}$$

$$J\frac{d\omega}{dt} + B\omega = \tau - T_L \tag{6}$$

A DFIM for wind applications is traditionally controlled in the stator flux orientation [10] or the natural flux/grid flux orientation [11]. In a propulsion application, e.g. on-board a ship with a fixed voltage and frequency AC service, ignoring winding resistance, the stator flux will be fixed in AC mode by the ship AC service. In this case, shaft torque can be controlled strictly from the rotor, and torque production is the only concern of the rotor inverter controller. In DC mode, stator flux can be controlled by both the stator current and also the rotor current. This complicates torque control, as the rotor inverter must ensure both a desired stator flux level and then command necessary torque. To make effective control possible in both modes, it makes sense therefore to model the machine in a reference frame oriented to the stator flux. This ensures that the control development will track the stator flux and therefore torque production in both modes and while transitioning between modes. This choice of reference frame also ensures that it is possible to synchronize a "bumpless" transition between modes while accelerating or decelerating the machine through the mode transition, as will be shown shortly.

Equations (1-5) are thereby transformed to the stator flux reference frame for control development. The stator flux is oriented towards the d-axis, and the q-axis leads it by 90°. The electrical dynamics of the system are governed by:

$$\frac{d}{dt}\psi_s = V_{sd} - R_s I_{sd} \tag{7}$$

$$\frac{d}{dt}\psi_{rd} = V_{rd} - R_r I_{rd} + \left(\omega_s - \omega_e\right)\psi_{rq} \tag{8}$$

$$\frac{d}{dt}\psi_{rq} = V_{rq} - R_r I_{rq} - \left(\omega_s - \omega_e\right)\psi_{rd} \tag{9}$$

$$\omega_s = \frac{d\theta_s}{dt} = \frac{V_{sq} - R_s I_{sq}}{\psi_s} \tag{10}$$

while the electromagnetic torque is governed by:

$$\tau = -\frac{2}{3}\frac{P}{2}\frac{M}{L_s}\psi_s I_{rq} \tag{11}$$

and the flux linkage equations are:

$$\psi_s = L_s I_{sd} + M I_{rd} \tag{12}$$

$$0 = L_s I_{sq} + M I_{rq} \tag{13}$$

$$\psi_{rd} = L_r I_{rd} + M I_{sd} \tag{14}$$

$$\psi_{rq} = L_r I_{rq} + M I_{sq} \tag{15}$$

IV. CONTROL ARCHITECTURE

The control architecture for the proposed drive is shown in Fig 2. Estimates of ψ_s and θ_s are used to transform relevant variables to the stator flux reference frame. The transition command ('Sw*') is generated based on the chosen speed for transitioning between AC and DC modes which is fed to a

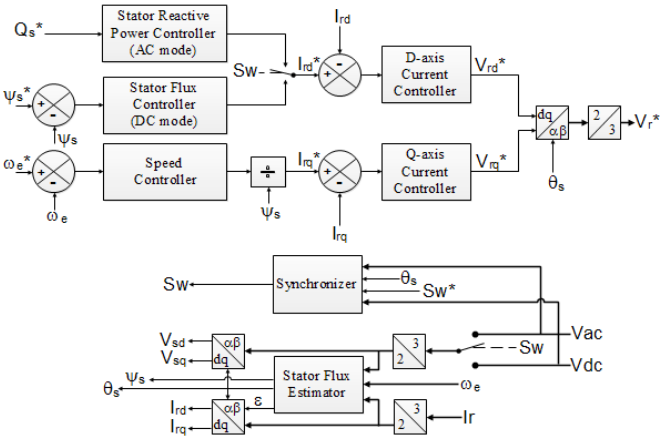

Figure 2. Control architecture of the proposed DFIM drive

synchronizer along with the stator flux angle, the AC and the DC voltages. The role of the synchronizer is to determine the correct instant of switching ('Sw') between AC and DC modes such that the stator flux is perturbed as little as possible, facilitating smooth or "bumpless" torque production given design limitations on the rotor power electronics. Full mechanical control of the DFIM is achieved from the rotor, and therefore power electronics are included in the controller for modifying the rotor d and q axis currents. The rotor q-axis current can be slaved to the command of a torque or speed loop. The rotor d-axis current performs different functions during the two modes. In DC mode, it influences the stator flux and it is thereby used to maintain the stator flux magnitude. In AC mode, it is used not only to control stator reactive power, but also to act as an active damper to suppress oscillations in the stator flux during transition. Thus, based on 'Sw', I_{rd}* is generated from either the stator reactive power controller or the stator flux controller. 'Sw' also controls the algorithmic computation of stator flux as appropriate for the two different modes. In the following section, each of these modules will be discussed in details.

A. Stator Flux Estimation

The most important aspect of stator flux oriented control is the estimation of stator flux itself; both in magnitude and phase under all operating conditions. In a DFIM, stator flux is generally estimated either through a voltage model based on the machine differential equations, a current model based on the flux linkage equations, or indirectly by a stator voltage vector i.e., a natural field orientation assumption regarding the phase of observed voltage and estimated flux [10]. As the proposed drive configuration undergoes stator voltage and flux transients, the stator voltage vector is inconvenient for stator flux estimation. The voltage model incorporates integrators in the stationary reference frame as in (16).

$$\psi_{s\alpha} = \int \left(V_{s\alpha} - R_s I_{s\alpha}\right) dt$$
$$\psi_{s\beta} = \int \left(V_{s\beta} - R_s I_{s\beta}\right) dt \qquad (16)$$

In AC mode, the integrators can be approximated with low pass filters in practical implementations [12], avoiding problems with offset and drift in the integral computations. The cutoff frequency of these low-pass filters must be well below the signal frequency. However this approximation of the integral with a low pass filter remains impractical in DC mode, where the signal frequency is zero.

The entire estimation problem in both modes can be greatly simplified by computing the stator flux with a hybrid estimator that uses flux linkage equations (a current model) augmented with voltage information from the stator, which must be measured in the DFIM controller anyway for synchronization.

For stator flux estimation, the stationary reference frame ($\alpha\beta$) is used. Using (2) in (1) to replace stator current,

$$\overline{V_s} = \frac{R_s}{L_s}\left(\overline{\psi_s} - M\overline{I_r}e^{j\varepsilon}\right) + \frac{d}{dt}\overline{\psi_s} \qquad (17)$$

The rotor current in the stationary reference frame is governed by:

$$I_{r\alpha} + jI_{r\beta} = \overline{I_r}e^{j\varepsilon} \qquad (18)$$

Using (18) in (17) and rearranging real and imaginary parts,

$$\frac{d}{dt}\psi_{s\alpha} + \frac{R_s}{L_s}\psi_{s\alpha} = V_{s\alpha} + \frac{R_s M}{L_s} I_{r\alpha}$$
$$\frac{d}{dt}\psi_{s\beta} + \frac{R_s}{L_s}\psi_{s\beta} = V_{s\beta} + \frac{R_s M}{L_s} I_{r\beta} \qquad (19)$$

These expressions for the components of stator flux are governed by first order differential equations that correspond to "low-pass" transfer functions relating the "input" voltages and currents to the "output" fluxes. This flux estimator is attractive, as its low pass quality may minimize the effect of voltage and current measurement noise.

By avoiding the direct use of stator current in the flux estimator, we preserve a mechanism for potentially detecting parameter variations as the machine operates. If stator currents are also measured, a second estimate of stator flux can be made using the flux linkage equation (12). Disagreement between the two stator flux estimates can potentially be used to trigger the need for revising machine parameters while the machine is operating. This approach for updating the machine model in real time is being presently explored.

B. Design of the Rotor Current Control and Speed Compensator

As discussed earlier, both DC and AC mode require a feedback loop to control speed and power electronic controls for the d and q axis rotor currents. The q-axis current controller can be designed using (15) and (13) to find ψ_{rq} in terms of I_{rq} and thereby substituting the result in (9). The equation governing the q-axis rotor current dynamics is:

$$V_{rq} = R_r I_{rq} + \left(L_r - \frac{M^2}{L_s}\right)\frac{d}{dt} I_{rq} + \left(\omega_s - \omega_e\right)\psi_{rd} \qquad (20)$$

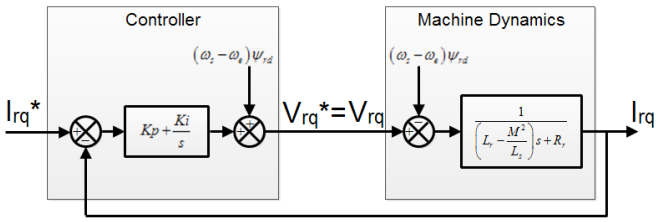

Figure 3. Block diagram for the design of q-axis current controller

The drive V_{rq} is provided by the rotor inverter. The desired V_{rq}^{*} is computed as the output of a PI compensator added to a speed voltage term that cancels the effect of ψ_{rd} in (20). ψ_{rd} is indirectly estimated using (12) and (14) as:

$$\psi_{rd} = \left(L_r - \frac{M^2}{L_s}\right) I_{rd} + \frac{M}{L_s}\psi_s \tag{21}$$

Figure 3 shows the overall q-axis current controller. Proportional and integral gains are chosen to ensure loop stability, desired transient response, and acceptable steady state error.

The design of the d-axis current controller is similar. (21) and (7) are used in (8), which is translated to measured or estimated variables using (12)-(15) to obtain:

$$V_{rd} = \left(R_r + \frac{R_s M^2}{L_s^2}\right) I_{rd} + \left(L_r - \frac{M^2}{L_s}\right)\frac{d}{dt} I_{rd} + \underbrace{\frac{M}{L_s} V_{sd} - \frac{R_s M}{L_s^2}\psi_s - (\omega_s - \omega_e)\left(L_r - \frac{M^2}{L_s}\right) I_{rq}}_{\text{Equivalent Voltage Terms}} \tag{22}$$

This equation is used to design a d-axis current controller with a PI compensator. The 'equivalent voltage' terms are added to the PI compensator output.

Finally, the shaft speed control is designed using (6) and by noting that the electromagnetic torque is related to the q-axis rotor current through (11). The bandwidth of the speed controller is chosen such that it is much slower than the q-axis current controller bandwidth. This is a design choice that will determine the final performance of the propulsion drive. A PI compensator stabilizes the speed loop in the experiments presented in this paper.

C. Flux Controller in DC mode

As mentioned earlier, the stator flux of the machine can be controlled strictly through the rotor, but only in DC mode. Using (12) in (7),

$$I_{rd} = \frac{L_s}{MR_s}\frac{d}{dt}\psi_s + \frac{1}{M}\psi_s - \underbrace{\frac{L_s}{MR_s} V_{sd}}_{\text{Voltage term}} \tag{23}$$

A PI compensator responsive to estimated flux error is used along with the voltage term to control the direct axis rotor current and therefore stator flux. The previously discussed rotor d-axis current compensator is a minor loop within the stator flux feedback compensator. Therefore, the bandwidth of the flux controller is chosen such that it is significantly lower than the d-axis current controller.

D. Synchronizer

The determination of the proper instance of transition between AC and DC modes is critical to incur minimal transients in the machine flux and speed during the change.

1) DC to AC Transition

The development of the synchronizer can be understood by imagining the DFIM operating in DC mode and switching to AC mode. Assuming the DFIM is operating steadily, V_{sd} and V_{sq} are the d-axis and q-axis components of the DC voltage in the stator flux reference frame as shown in Fig. 4. These are stationary since the stator flux itself is stationary. The AC voltage vector (V_{ac}) represents the to-be-connected ship service AC mains. This vector is transformed to the stator flux reference frame, and rotates counter-clockwise at the AC supply frequency.

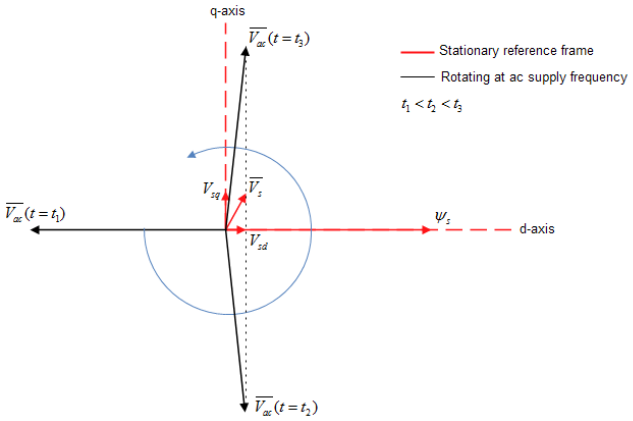

Figure 4. Space vector diagram for DC to AC transition

For minimal perturbation of the stator flux magnitude at the instant of switching, the d-axis component of AC voltage must be equal to V_{sd} as governed by (7). This gives two instances, t_2 and t_3, for transition. However, the stator flux frequency must move from zero to the AC supply frequency after the transient which is governed by (10). A positive q-axis component of AC voltage drives the stator flux frequency towards the AC supply frequency. As will be confirmed in our simulations and experimental results, switching at t_3 ensures that the model-transition is accomplished as quickly as possible and with minimal disturbance to the stator flux.

2) AC to DC Transition

During the AC to DC transition, V_{sd} and V_{sq} are initially the d-axis and q-axis components of the AC voltage in the stator flux reference frame as shown in Fig. 5. However, now the DC voltage vector V_{dc} rotates clockwise at the AC supply frequency when transformed to the stator flux reference frame. Using the same argument as in the DC to AC transition, matching the d-axis component of the DC voltage with V_{sd} and ensuring that the q-axis component of the DC voltage is negative or zero makes t_3 the optimum switching instant from AC to DC.

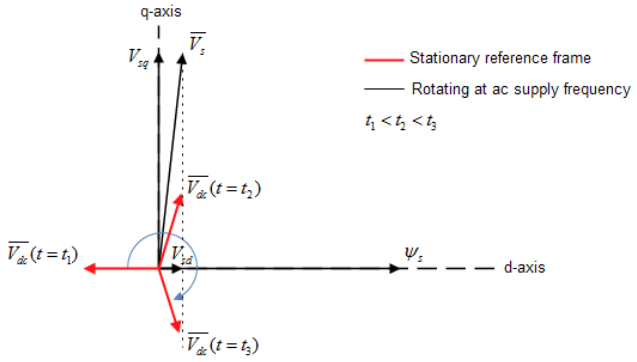

Figure 5. Space vector diagram for AC to DC transition

A flowchart of the synchronizer scheme is shown in Fig. 6 that pulls these two observations about the transition between modes together. Based on the 'Sw*' command, 'Sw' is generated. When in DC mode, a command to connect the stator to AC will set the Q bit of the RS latch. When in AC mode, a command to connect the stator to DC will reset the bit at the appropriate instant.

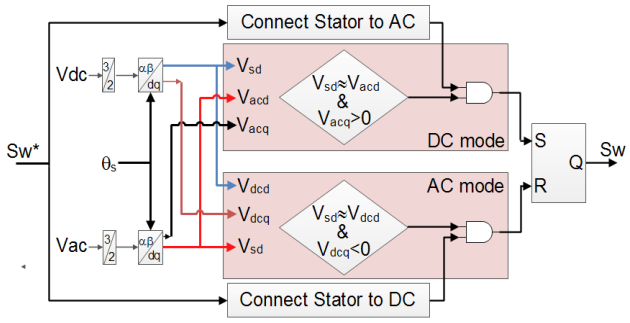

Figure 6. Flowchart of Synchronizer

E. Steady State Reactive Power Control in AC Mode

In AC mode steady-state operation, the stator flux is determined by the mains AC voltage and frequency. Assuming a negligible stator resistance in (7) and (10),

$$\psi_s = \frac{V_{sq} - R_s I_{sq}}{\omega_s} \approx \frac{V_{sq}}{\omega_s} \approx \frac{\left|\overline{V_{ac}}\right|}{\omega_{ac}} \tag{24}$$

Thus, the flux controller in DC mode is deactivated and instead, the d-axis rotor current can now be used to control the flow of reactive power to and from the AC mains as in a standard wind turbine application [13]. Any desired stator reactive power within the machine and inverter limits can be provided according to:

$$Q_s = \frac{2}{3}\frac{P}{2}\left(V_{sq} I_{sd} - V_{sd} I_{sq}\right) \tag{25}$$

Substituting stator current components in terms of rotor currents using (12) and (13), this expression for reactive power can be expressed as

$$Q_s = \frac{2}{3}\frac{P}{2}\left(\frac{V_{sq}\psi_s}{L_s} + \frac{MV_{sd} I_{rq}}{L_s} - \frac{MV_{sq}}{L_s} I_{rd}\right) \tag{26}$$

Rearranging, the required rotor d-axis current necessary to command the steady-state reactive power flow on the stator can be computed as:

$$I_{rd}^{\ *} = \left(\frac{1}{M}\psi_s + \frac{V_{sd}}{V_{sq}} I_{rq} - \frac{3}{P}\frac{L_s}{MV_{sq}} Q_s^{\ *}\right) \tag{27}$$

F. Transition to AC mode

When transitioning from AC mode to DC mode, the stator flux will be maintained by the previously discussed flux controller. When transitioning from DC to AC mode, the extra degree of freedom available through I_{rd}, exploited above to command stator reactive power in steady-state operation, will, if uncontrolled during a transient, lead to a disturbance in the stator flux. This transient could also be excited by differences in the magnitude of the initial stator flux in DC mode and the final flux magnitude just after the transition to AC mode. The rotor d-axis current can also be used to control this transient response when switching to AC mode.

Assuming V_{sq} is much higher than the resistive drop, a simplified non-linear model can be developed from the AC supply frequency to stator flux. Rearranging (23),

$$\frac{L_s}{R_s}\frac{d}{dt}\psi_s + \psi_s = MI_{rd} + \frac{L_s}{R_s} V_{sd} \tag{28}$$

Simplifying (10),

$$V_{sq} = \omega_s \psi_s \tag{29}$$

The instantaneous angle between the stator flux reference frame and AC voltage reference frame rotating at AC supply frequency, δ, can be computed as:

$$\frac{d\delta}{dt} = \omega_{ac} - \omega_s ; \tan\delta = \frac{V_{sq}}{V_{sd}} \tag{30}$$

and of course, the total AC voltage vector magnitude equals the resultant from the d-axis and q-axis components.

$$V_{sd}^{\ 2} + V_{sq}^{\ 2} = \left|\overline{V_{ac}}\right|^2 \tag{31}$$

The non-linear model described by (28)-(31) is represented graphically in Fig. 7. If $I_{rd}^{\ *}$ is set to zero or any value based on (27), after transition from DC to AC mode, a step change in ω_{ac} results in flux oscillations. The use of a feedback damper with a gain K_d to suppress the flux oscillations is currently under experimentation. This will be shown to be effective empirically in the experimental results.

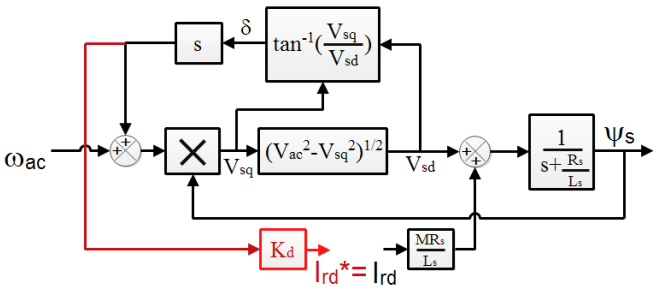

Figure 7. Non-linear model relating ω_{ac} to ψ_s during transition from DC to AC mode and inclusion of proposed feedback gain (in red) [$I_{rd}^* = I_{rd}$ is assumed using high bandwidth approximation]

Thus, the complete reactive power controller and transition flux controller are augmented together to dampen out the stator flux oscillations and control the stator reactive power. Fig. 8 shows the complete integrated AC reactive power controller, the output of which is fed to the rotor d-axis current controller in AC mode. Formal stability analysis of this is under investigation, but good results have been found empirically.

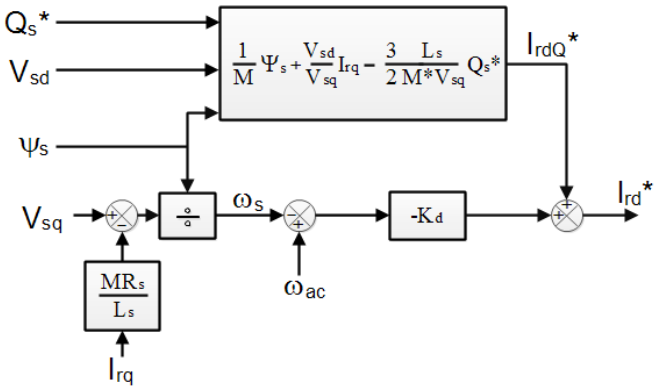

Figure 8. Integrated AC mode reactive power controller

V. Simulation & Experimental Results

A 1 HP, 220 V/ 150 V, 60 Hz, 4 Pole DFIM has been used to illustrate the control architecture experimentally. Two Texas Instruments High Voltage Motor Control & PFC Developer's Kits, named Kit-I and Kit-II, are used for this purpose. The stator is connected to Kit-I, and is programmed to operate either as a DC source or a fixed frequency fixed voltage AC source. The rotor is connected to Kit-II, and is used as a variable frequency drive. When emulating an AC supply, Kit-I is programmed to supply 28 V, 12 Hz, and maintains a voltage of 8 V when emulating a DC source. Although this would not be the case in an actual implementation, this setup is chosen for demonstration only. The DFIM is also mechanically coupled to a Permanent Magnet Synchronous Generator (PMSG) which is connected to a programmable load bank. Additionally, a MATLAB™ Simulink model is used to illustrate the effect of unsynchronized switching between the AC and DC modes.

A. *Evaluation of Synchronizer and Correct Instant of Transition in Simulation*

The synchronizer algorithm is tested in simulation, and the results for a DC to AC transition at a constant speed are shown in Fig. 9. If the transition is made at the correct instant as determined by the synchronizer, minimal perturbation in the stator flux magnitude is observed compared to when the transition is delayed. The normalized stator flux magnitude is supposed to remain as constant as possible. In a practical scenario, a large perturbation in stator flux can result in complete loss of synchronism.

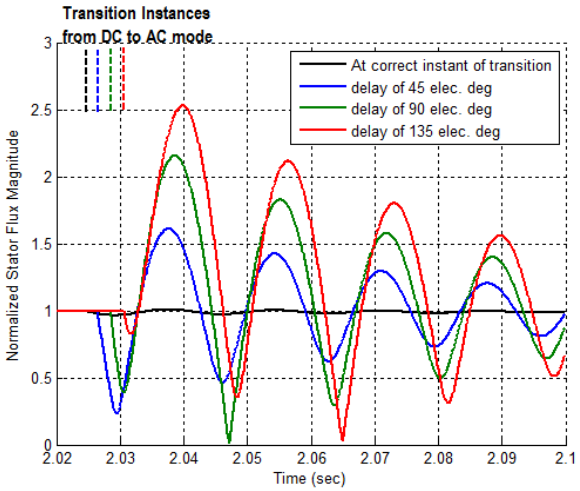

Figure 9. Simulation result: Effects of unsynchronized switching from DC to AC mode [nomalized to stator flux magnitude during the DC Mode]

B. *Experimental Evaluation of the Dynamic Performance of the Overall Controller*

For the experimental setup, the transition speed is set to 180 rpm. That is, when the speed goes above 180 rpm, Sw* is commanded to apply the AC supply to the stator. When the speed goes below 180 rpm, Sw* is commanded to apply the DC supply to the stator. The AC supply synchronous speed is 360 rpm.

1) *Performance of the Controller during Acceleration*

To evaluate the performance of the complete controller, a step command in speed of 540 rpm is given under three different conditions as shown in Fig. 10. In the first condition, neither the reactive power controller nor the stator flux transition controller are used in the loop, which implies that after the transition to AC mode, I_{rd}^* is set to zero. Figure 10(b) illustrates the electromagnetic torque and the estimated stator flux as speed ramps up and the operating mode changes from DC mode to AC mode near t=0.5 sec. There are significant oscillations in estimated stator flux as well as in torque. Since I_{rq} is limited to its maximum value during aceleration, oscillations in stator flux estimation are reflected in the electromagnetic torque, and the torque controller cannot dampen out these oscillations. Also, differences in the stator flux magnitude during DC mode and AC mode result in differences in the electromagnetic torque during the two modes. Therefore, the slopes of the speed acceleration curves for DC mode and AC mode are different. Also, it is important

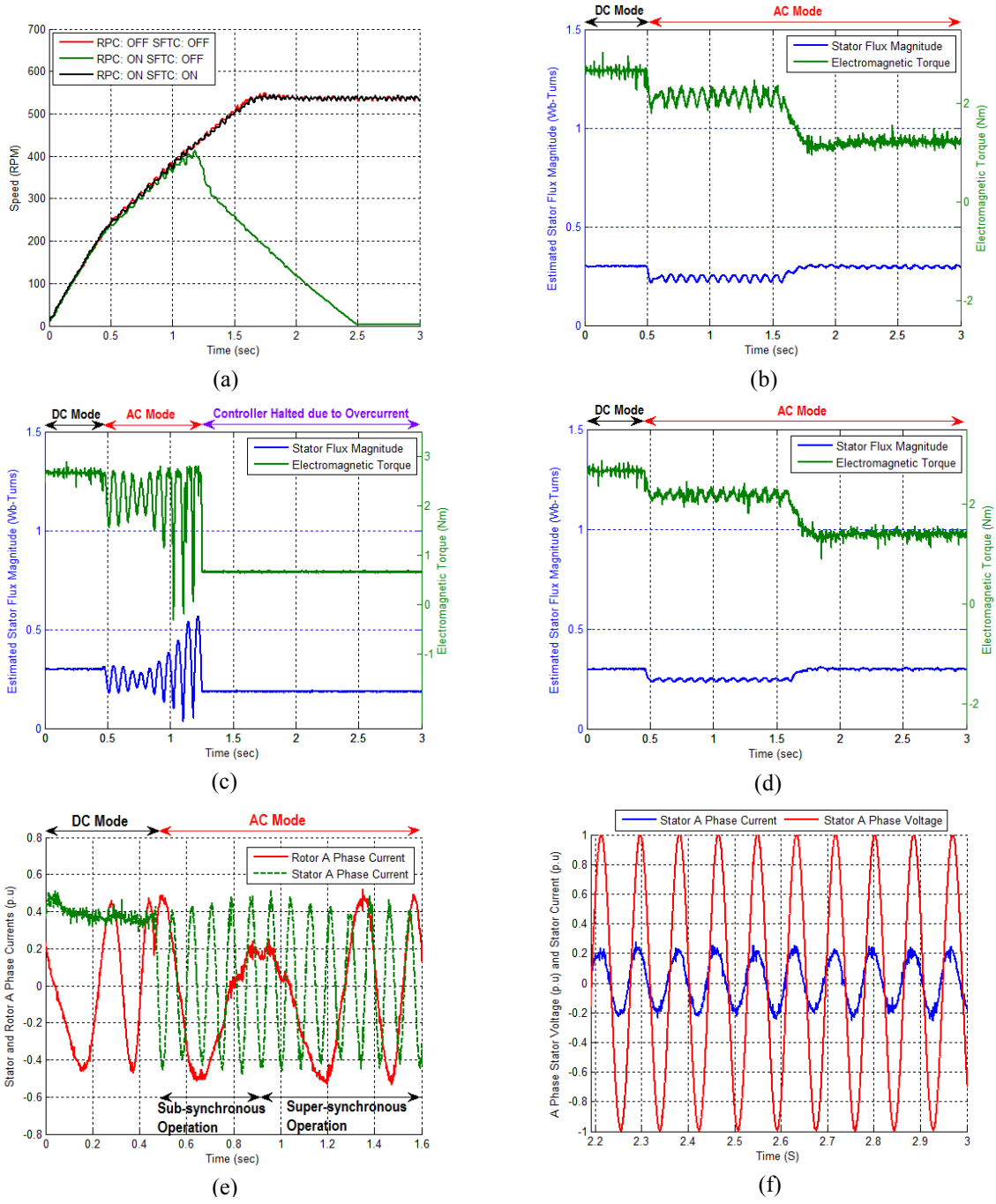

Figure 10. Experimental Results: (a) Actual speed with a commanded speed of 540 rpm (b) Estimated stator flux magnitude and electromagnetic torque without RPC or SFTC (c) Estimated stator flux magnitude and electromagnetic torque with RPC and without SFTC (d) Estimated stator flux magnitude and electromagnetic torque with RPC and SFTC (e) Stator A phase and Rotor A phase current with RPC and SFTC during acceleration (f) A phase voltage and current at 540 rpm with RPC and SFTC enabled

to observe that though the transition speed is set at 180 rpm, the changeover takes place at around 220 rpm. The delay is due to the functional synchronizer that causes a delay between Sw* and Sw (which determines the actual transition between modes). In the second condition, shown in Fig. 10(c), a speed command is given with only the reactive power controller (RPC) enabled in AC mode. This implies that only I_{rdQ}* is used to command I_{rd}*. With no stator flux transition controller (SFTC), after the transition to AC mode, the DFIM looses synchronism and comes to a halt due to over current protection in Kit-II. As the controller trips due to over current protection, the estimated values of stator flux and electromagnetic torque are set to their last registered values before the trip.

Finally, in the third condition, both SFTC and RPC are enabled in the controller loop. In steady state, zero reactive power is drawn from the stator as shown in Fig. 10(f) because Q_s* is set to zero. The stator voltage and current are normalized to the AC supply voltage and the rated current of the stator, respectively. The presence of the SFTC not only allows the use of the RPC in AC mode, but also lowers the

stator flux and thereby electromagnetic torque oscillations after the transition as shown in Fig. 10(d). Fig 10(e) shows the p.u stator current and rotor current normalized to their rated values as the speed ramps up.

2) Dynamic Performance of the Controller for Reference Speed Tracking

Three sets of alternating reference speed commands are given as inputs to the controller as shown in Fig. 11. First, the reference speed alternates between 75 rpm and 120 rpm. This regime is entirely in DC mode. In the second set, the reference speed alternates between 320 rpm and 400 rpm. This regime is entirely in AC mode. In the third set, the reference speed alternates between 150 rpm and 210 rpm. In this test, the controller switches between AC and DC modes based on the actual speed. A programmable load bank is turned on for each set of tests around 7.5 sec. As the DFIM is connected to a PMSG, the voltage generated by the PMSG and thereby the load on the DFIM increase with speed. That is, the load has more of an effect on acceleration at a higher speed than it does at a lower speed.

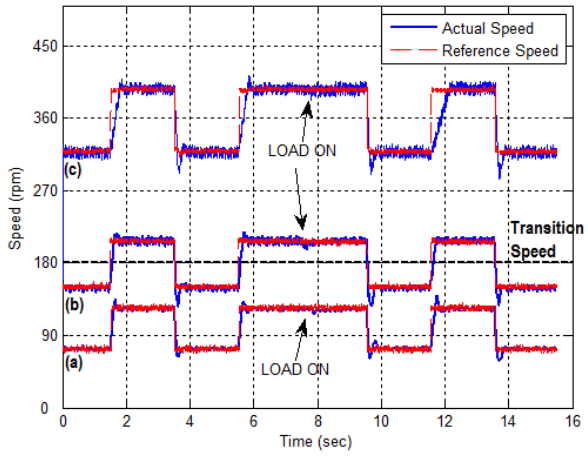

Figure 11. Experimental Results: Reference tracking of speed controller in three speed ranges - (a) DC Mode only (b) DC and AC modes (c) AC mode only

TABLE I. DFIM PARAMETERS

Stator resistance	3.575 Ω
Rotor resistance	4.229 Ω
Stator leakage inductance	9.6 mH
Rotor leakage inductance	9.6 mH
Mutual inductance	165 mH
Moment of inertia	0.01 kgm^2
Frictional coefficient	0.0025 Nm-s/rad

VI. CONCLUSION

This paper discusses and demonstrates control architecture for a DFIM suitable for a propulsion application where both AC and DC power are available. With a proper choice of transition speed, the proposed configuration can enable full speed range for the drive with minimal power electronics. The results show that the proposed controller works equivalently under the tested operating conditions (DC mode, AC mode, and when transitioning between AC and DC modes). The results also validate the operation of the stator flux estimator, synchronizer, reactive power controller and stator flux transition controller. A more robust controller may include an on-line parameter estimation scheme to update not only the DFIM parameters, but also tune the controller for variable load friction and inertia. Finally, proper switching between DC and AC modes and a controlled flux transition for reactive power control (in AC mode) open up opportunities for system level design choices to be made that can minimize weight and cost of the propulsion drive.

ACKNOLEDGEMENT

This research was performed with support from the Electric Ship Research and Development Consortium under The Office of Naval Research. This work was also in part supported by The Grainger Foundation.

REFERENCES

[1] J. S. Chalfant, C. Chryssostomidis, M. G. Angle "Study of parallel AC and DC electrical distribution in the all-electric ship", *Proc. Conference on Grand Challenges in Modeling & Simulation*, pp. 319-326, 2010

[2] F. Blaabjerg, M. Liserre and Ke Ma, "Power Electronics Converters for Wind Turbine Systems", *IEEE Trans. Ind. Applicat.*, vol. 48, no. 2, pp. 708-719, Mar/Apr 2012.

[3] H. Akagi and H.Sato, "Control and Performance of a Doubly-Fed Induction Machine Intended for a Flywheel Energy Storage System", *IEEE Trans. Power Electron.*, vol. 17, no. 1,pp 109-116, Jan 2002 .

[4] Y. Kawabata, E. Ejiogu and T. Kawabata, "Vector-controlled double inverter-fed wound-rotor induction motor suitable for high-power drives", *IEEE Trans. Ind Appl.*, vol. 35, no. 5, pp. 1058–1066, Sep./Oct. 1999.

[5] G.Poddar and V. T. Ranganathan, "Sensorless field-oriented control for double-inverter-fed wound-rotor induction motor drive", *IEEE Trans. Ind. Electron.*, vol. 53, no. 1, Feb 2006.

[6] S. B. Leeb et al. , "How much dc power is necessary?", *Nav. Eng. J.*, vol. 122, no. 2, pp. 79–92, Jun. 2010.

[7] R. Pena, J.C. Clare and G.M. Asher, "Doubly-fed induction generator using back-to-back PWM converters and its application to variable-speed wind-energy generation", *IEE Proc., Electr. Power. Appl.*, 143, (3), pp. 231-241, 1996.

[8] A. Tapia, G. Tapia, J. Ostolaza, and J. Saenz, "Modeling and control of a wind turbine driven doubly fed induction generator", *IEEE Trans. Energy Convers.*, vol. 18, no. 2, pp. 194–204, Jun. 2003.

[9] W. Leonhard, Control of Electrical Drives. Berlin, Germany: SpringerVerlag, 1985.

[10] B. Hopfensperger, D. J. Atkinson, and R. A. Lakin, "Stator-flux-oriented control of a doubly-fed induction machine with and without position encoder", *Proc. Inst. Elect. Eng., Electr. Power Appl.*, vol. 147, no. 4, pp. 241–250, Jul. 2000.

[11] A. Petersson, L. Harnefors, and T. Thiringer, "Comparison between stator- flux and grid-flux-oriented rotor current control of doubly-fed induction generators", in *Proc. 35th IEEE PESC*, Aachen, Germany, vol. 1, pp. 482–486, 2004.

[12] N. R. N. Idris and A. H. M. Yatim, "An improved stator flux estimation in steady-state operation for direct torque control of induction machines", *IEEE Trans. Ind. Appl.*, vol. 38, no. 1, pp. 110–116, Jan./Feb. 2002.

[13] L. Xu and W. Cheng, "Torque and reactive power control of a doubly fed induction machine by position sensorless scheme", *IEEE Trans. Ind. Appl.*, vol. 31, no. 3, pp. 636–642, May/Jun. 1995.